

Proposal of a method to observe road status using UAV considering post-disaster urgency based on mobile spatial dynamics data

Jun Sakamoto¹

Received: 24 February 2025 / Accepted: 19 May 2025

Published online: 26 May 2025

© The Author(s) 2025 OPEN

Abstract

Disasters can lead to bridge collapses, road flooding, and mudslide blockages, disrupting the road network and hindering victims' movement and rescue operations. After a disaster, it is crucial to quickly assess the damage and identify access routes to affected areas to transport relief supplies and conduct rescue operations. Recent advances in digital transformation (DX) technology have the potential to revolutionize disaster management planning. Uncrewed Aerial Vehicles (UAVs) are being utilized to assess damage, while GPS data from mobile phones is helping to visualize evacuation behavior. The goal of this research is to enhance community resilience, minimize damage and enable rapid recovery by improving emergency response after a disaster. We propose a method for efficiently observing road damage after a disaster using population flow data derived from UAV and GPS data. The method focuses on assessing concentrated population areas, touring from one evacuation center to another based on the road network. We employ the Traveling Salesman Problem (TSP) and route search methods to calculate distances between points. The proposed model was applied to the Mabi city, Kurashiki City, Okayama Prefecture, which suffered significant damage during the July 2018 rainstorm. Results indicate that the proposed method can effectively gather data on road blockages in areas with higher population densities than static census data. Additionally, it found that investigating the flooding situation of roads at that time through land routes, such as vehicles, proved challenging because many routes connecting densely populated areas to evacuation centers were continuously flooded.

Keywords UAV · Mobile phone data · TSP · GIS

1 Introduction

Disasters are unexpected events, and their impact on the local area is uncertain [1]. Disasters can cause the collapse of bridges, flooding of roads, and the blocking of roads by mud and sand, which can disrupt the road network. Impassable roads due to disasters can affect the movement of disaster victims and rescue activities [2]. After a disaster, it is crucial to quickly identify the damaged areas and determine routes to access them to provide relief and rescue victims [3]. In the case of a large-scale disaster, multiple areas may be affected, and many routes could be blocked. It is important to create flexible plans that consider the disaster's scale, even during regular times, to expedite road restoration after a disaster [4].

Recent technological advancements have increased attention to disaster response utilizing UAVs (uncrewed aerial vehicles) [5]. Numerous studies have focused on damage assessment using images captured by UAVs. These studies have addressed various scenarios, including forest fire detection [6], road damage caused by earthquakes [7], and assessment of flood extent [8]. The data from these analyses is typically categorized into two types: oblique photographs and

✉ Jun Sakamoto, jsak@kochi-u.ac.jp | ¹Faculty of Science and Technology, Kochi University, Kochi, Japan.



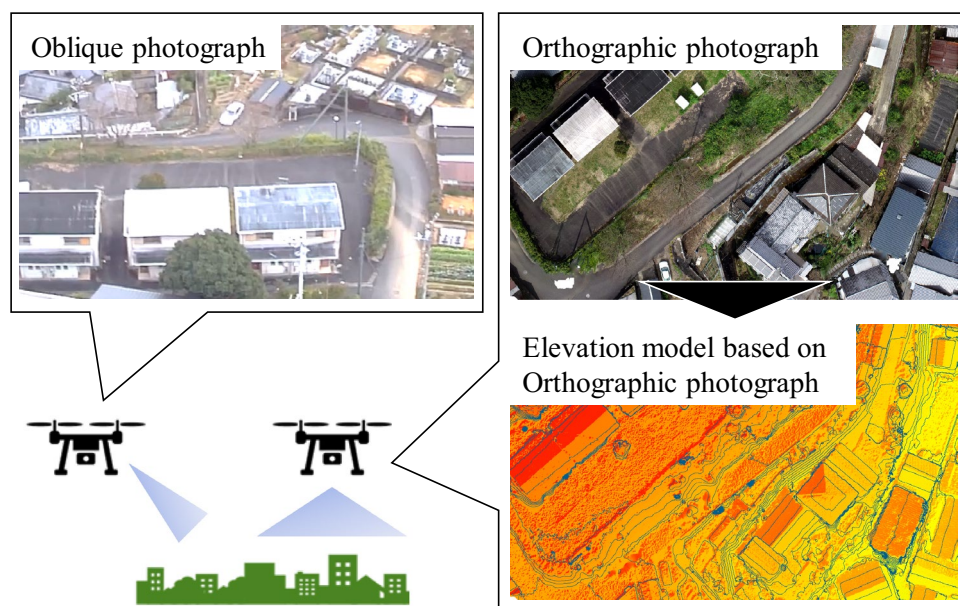
orthographic photographs, as illustrated in Fig. 1. Oblique photographs can capture data over a wide area but require additional analysis since they are often less straightforward to interpret. In contrast, orthographic photographs have a narrower field of view but can be converted into digital elevation models and other formats, allowing for more detailed analysis. Research on optimizing UAV flight routes includes methods for developing flight paths based on pre-disaster information and techniques for monitoring closed roads during emergencies [9–11].

The increasing use of mobile devices has led to the application of location data from mobile phones in disaster response efforts [12]. Research focusing on the immediate aftermath of a disaster includes the development of smartphone applications to aid in evacuation and studying evacuation behaviors [13–15]. In addition, research examining the entire process from disaster to recovery and reconstruction analyzes patterns of population decline in affected areas [13, 16]. It quantifies recovery by tracking the number of visitors to recovery facilities [17]. As demonstrated, location data from mobile phones has significant potential for various disaster response scenarios.

This research proposes a new method for prioritizing road repairs immediately after a disaster using UAVs and mobile phone data. The method efficiently surveys roads between densely populated areas and evacuation centers following a disaster. It contributes to rapidly assessing road blockage status using the orthographic photograph obtained during the patrols. Disaster response has two phases: preparation during peacetime and response following a disaster [18]. Peacetime preparation involves planning based on existing information. In contrast, a response occurs in an unpredictable environment after a disaster [19]. The feature of the proposed model is to combine peacetime preparation, such as knowledge of road networks and the locations of evacuation centers, with the determination of patrol routes based on population flow data immediately after a disaster. The proposed model utilized in this research is a straightforward approach that employs the Traveling Salesman Problem (TSP). Its purpose is not to analyze routing methods rigorously. Instead, it aims to explore new possibilities for disaster response by integrating GPS data from UAVs and mobile phones, along with information about road networks and evacuation centers. It would be best to visit all target areas and take orthographic photographs of everything [20]. However, local governments often operate versatile UAVs with battery limitations, making it challenging to fly them for extended periods [21]. This research aims to develop a method for prioritizing the assessment of road conditions between disaster response center, evacuation centers, and densely populated areas.

This study verifies the proposed method in a specific case study area that has experienced torrential rain disasters, for mobile phone data is available. It examines multiple periods immediately following a disaster and develops patrol routes based on population flow data collected at each time point. When road administrators have not yet fully assessed the damage, and it is challenging to survey the area on the ground, this method aims to gather information that enables more individuals to reach evacuation shelters quickly by utilizing UAVs. We conduct the following verification to demonstrate the significance of the proposed model for patrol routes. Specifically, we compare routes generated using dynamic data,

Fig. 1 Method for capturing images using a UAV



such as population flow, with those created using static data, like census information. The evaluation focuses on whether the routes based on dynamic data can reach more people immediately after a disaster than those based on static data.

Natural disasters result in significant economic and human losses, undermining sustainable development. Therefore, disaster risk reduction is crucial for achieving the Sustainable Development Goals (SDGs) [22]. The elements that make up disaster resilience include regional vulnerability, preventive measures, adaptive capacity, and transformative capacity [23]. This study focuses on adaptive capacity, aiming to reduce damage and improve regional resilience during a disaster.

The rest of the paper is structured as follows. Section 2 explains the methodology adopted in this study, the study area, and the data used. Section 3 highlights the results and discussion, and Sect. 4 presents the conclusions.

2 Methodology

2.1 Proposed model

Figure 2 illustrates an overview of the proposed method. This method assumes that an administrator utilizes sequentially updated population flow data to identify disaster-stricken areas that require assessment and repairs following a disaster. It also presents an efficient approach for patrolling these areas using UAVs, starting from disaster response center and extending to evacuation centers.

The data for the method are (1) disaster response center and evacuation centers designated as patrol bases and (2) road network data shown in Fig. 2a. As a preliminary step in calculating the patrol route, the model matches the disaster response center and evacuation center nodes with the nearest nodes in the road network data. Data for disaster response and evacuation centers is entered based on the disaster prevention plans created by local governments. The data utilized immediately after a disaster occurs consists of population flow data shown in Fig. 2b. This data helps determine the

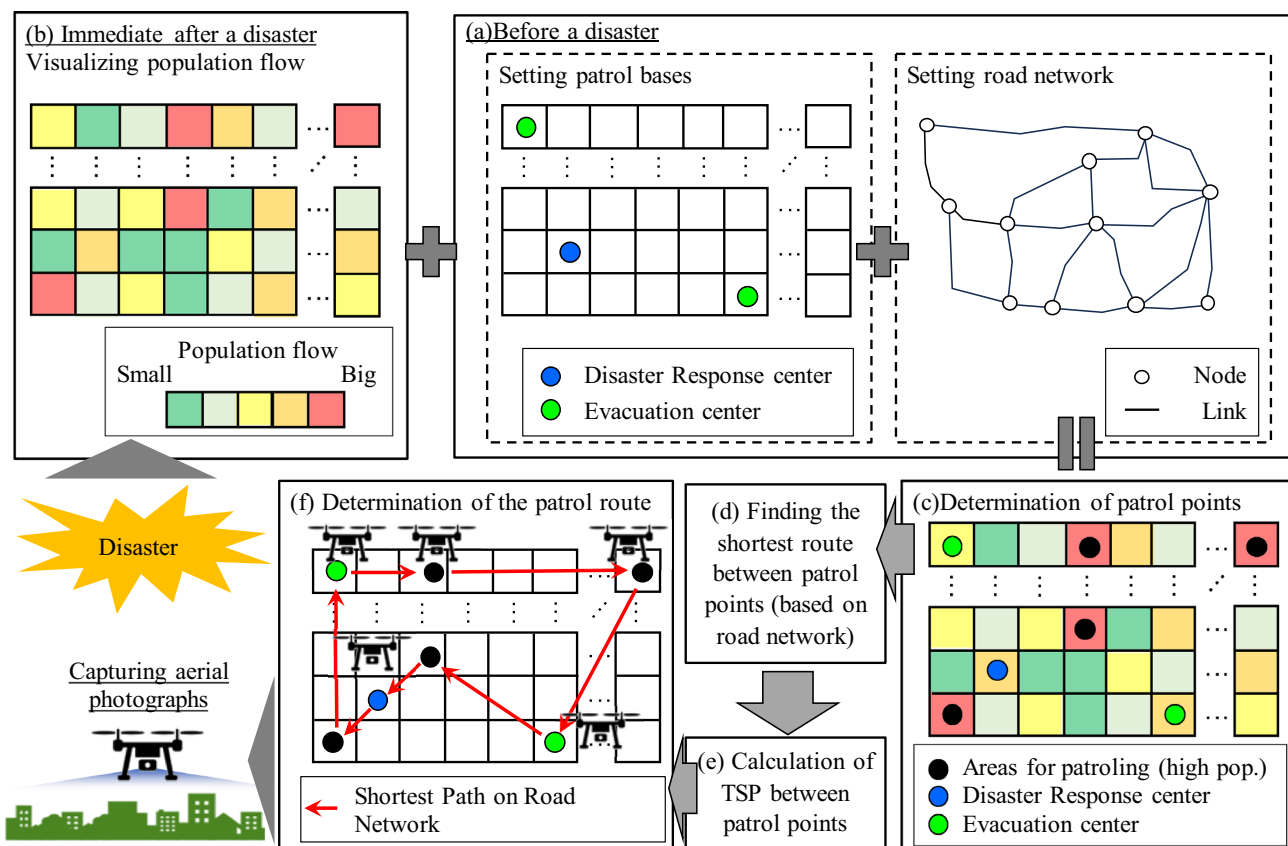


Fig. 2 Outline of proposed method

appropriate routes, requiring pre-matching between the mesh's centers of gravity and the road network's closest nodes. The node closest to each disaster response center and evacuation center is identified using GIS's spatial join function.

Immediately after a disaster is detected, the patrol area is determined as soon as the population flow data is available. Population flow data is provided in predefined mesh units. The disaster response center and evacuation centers are pre-established as bases and patrol points. The patrol points are identified using the population movement data, with the population ranked by mesh, designating the top meshes as "circulated disaster areas (population accumulation)" shown in Fig. 2c. The number of meshes used as patrol points depends on the UAV's performance and the range of its patrol. The centers of these meshes are then connected to the nodes of the road sections, facilitating a route search between the circulated areas.

Additionally, the node nearest to the center of gravity of each mesh is determined using GIS's spatial join function. The administrator calculates the shortest path search for all circulated road network areas for each origin–destination (OD) pair. It performs the shortest path search using MATLAB's "shortest path" function [24]. For example, if there are six locations to visit, the number of shortest path searches for each OD pair amounts to 15 routes (calculated as 6C2), shown in Fig. 2d. Utilizing this data, we employ the Dantzig–Fulkerson–Johnson (DFJ) approach [25] to address the Traveling Salesman Problem (TSP). Our goal is to solve a combinatorial optimization problem that minimizes the total travel cost of the route network connecting the disaster response center as a starting and ending point, as illustrated in Fig. 2e. This network includes evacuation shelters and disaster areas.

The nodes are labeled from 1 to n, with node one as the starting and ending points. Let us define x_{ij} as Eq. (1).

$$x_{ij} = \begin{cases} 1, & \text{if the path goes from node } i \text{ to node } j \\ 0, & \text{if } j = 1 \\ 0, & \text{otherwise} \end{cases} \quad (1)$$

c_{ij} represents the travel cost (distance) from node i to node j . Therefore, the shortest path problem can be expressed as an integer linear programming (ILP) problem shown in Eq. (2a).

$$\min Z = \sum_{i=1}^n \sum_{j \neq i, j=1}^n c_{ij} x_{ij} \quad (2a)$$

subject to

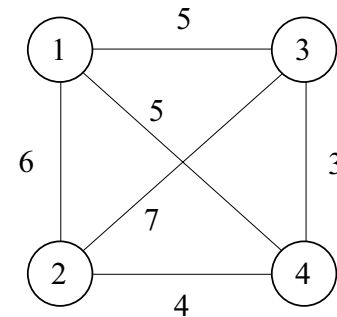
$$\sum_{i=1, i \neq j}^{n-1} x_{ij} = 1 \quad j = 1, \dots, n \quad (2b)$$

$$\sum_{j=2, j \neq i}^n x_{ij} = 1 \quad i = 1, \dots, n \quad (2c)$$

$$\sum_{i \in Q} \sum_{j \neq i, j \in Q} x_{ij} \leq |Q| - 1, \quad \forall Q \subseteq 1, \dots, n, |Q| \leq 2 \quad (2d)$$

The first constraint ensures that each node is visited once, the second guarantees that each node is departed from once, and the final constraint prevents the formation of partial tours. In this study, the travel cost refers to the shortest route between each node based on the road network. By solving this problem using TSP, we can determine the shortest path and its associated travel cost. The results of this calculation, visualized on GIS, represent the "shortest traveling route based on the road network" depicted shown in Fig. 2f.

Figure 3 delivers a simple network for understanding the calculation procedure of the proposed model. The numbers inside the circle represent node numbers, while the numbers between the nodes indicate travel costs. Starting from node one, the shortest route to return to 1 after visiting 2, 3, and 4 is 1 → 3 → 4 → 2 → 1, and the travel cost is 18. Expressing this in Eq. (2), we get $Z = c_{13}x_{13} + c_{34}x_{34} + c_{42}x_{42} + c_{21}x_{21} = 5 \times 1 + 3 \times 1 + 4 \times 1 + 6 \times 1$. In other words, x_{ij} is 0 for all routes other than the shortest.

Fig. 3 Example network

In summary, the model proposed in this study delivers a patrol route for monitoring road conditions connecting the centers of each mesh designated for inspection. The monitoring range can vary based on the performance of the UAV and the altitude at which it captures images. In other words, the route does not always capture the whole area of a mesh. However, there are cases where there is a noticeable concentration of road damage in a particular mesh. In that case, additional monitoring using UAVs is necessary to understand the situation.

2.2 Study area

This study focuses on Mabi town, located in Kurashiki City, Okayama Prefecture, in the Chugoku region of Japan shown in Fig. 4. As of December 2024, the population of the town is 20,252. The town is situated within the valley of the Takahashi River, a first-class river, and the Oda River, which is part of the Takahashi River system.

In July 2018, Mabi town experienced extensive damage due to record-breaking torrential rain. A low-pressure system formed from Typhoon Prapiroon merged with a stationary rain front near the main island of Japan on July 5, causing persistent heavy rainfall from July 5 to July 8. This intense rainfall primarily affected western Japan and the Tokai region, resulting in widespread flooding in Mabi town and leading to 51 fatalities. Fig. 5 illustrates the estimated color-coded map of the area around Mabi town, Kurashiki City, during the 2018 West Japan heavy rain [26]. It represents an estimate of the flooding depth provided by the Geographical Survey Institute based on flood marks, photographs, aerial images, and other records in the area. The embankments of the Oda River and other nearby rivers collapsed, leading to significant flooding in the city center, which is home to numerous houses and hospitals. The flood area reached its maximum extent of 1,200 hectares on July 7, 2018, but had reduced to approximately 500 hectares by July 9. Between July 8 and July 10, drainage efforts were undertaken by the Ministry of Land, Infrastructure, Transport, and Tourism, followed by road clearance work that began on July 10 [27, 28].

Research has highlighted that the low evacuation rate contributed to the high fatalities during the torrential rain disaster in Mabi Town in 2018. Various studies have utilized mobile phone location data and questionnaire surveys to map the

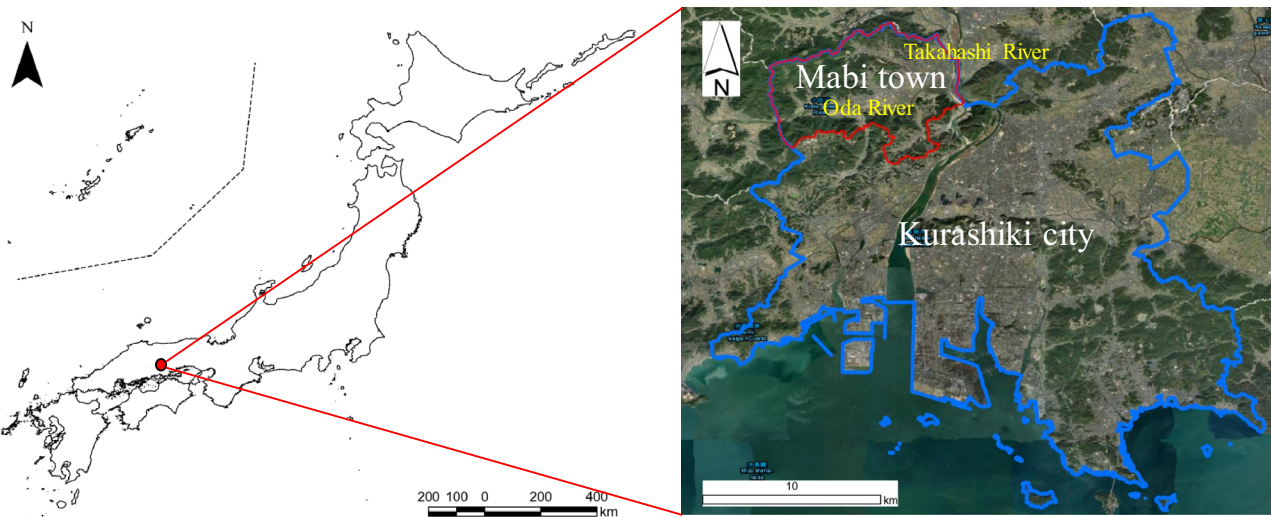
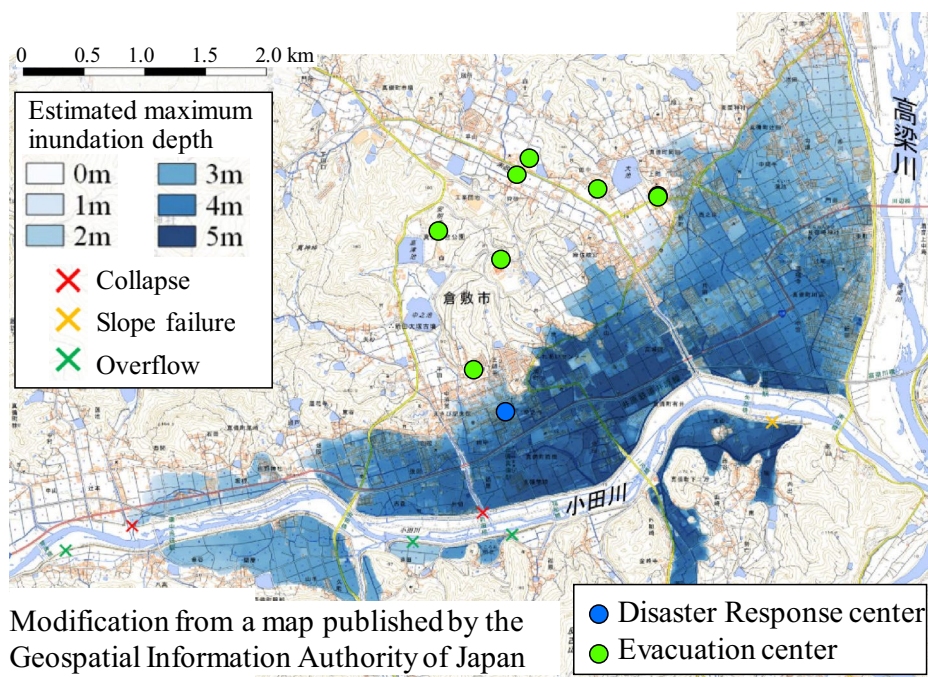
**Fig. 4** Location of Mabi town

Fig. 5 Estimated inundation depth



evacuation situation on the day of the disaster [29, 30]. Additionally, a study has focused on evacuation requests made through social networking services [31]. A study clarified that residents who were aware of flooding risks, as indicated by flood hazard maps, and those who participated in evacuation drills had a higher evacuation rate [32].

Given the extensive flooding in Mabi town, it is essential to gather information on whether residents who initiated horizontal evacuations immediately after the disaster could reach evacuation centers. Furthermore, during the emergency response phase, it is crucial to identify which roads are closed in order to facilitate road repairs. This research uniquely addresses these challenges using UAV and mobile phone data.

2.3 Data

Figure 6 illustrates the spatial data for the target area. The area consists of 205 mesh units corresponding to Mabi town. Kurashiki City's disaster response center is the Mabi branch office. Within the research target area, eight locations are designated by Kurashiki City as emergency evacuation sites and centers, which are also identified as evacuation centers during floods [33].

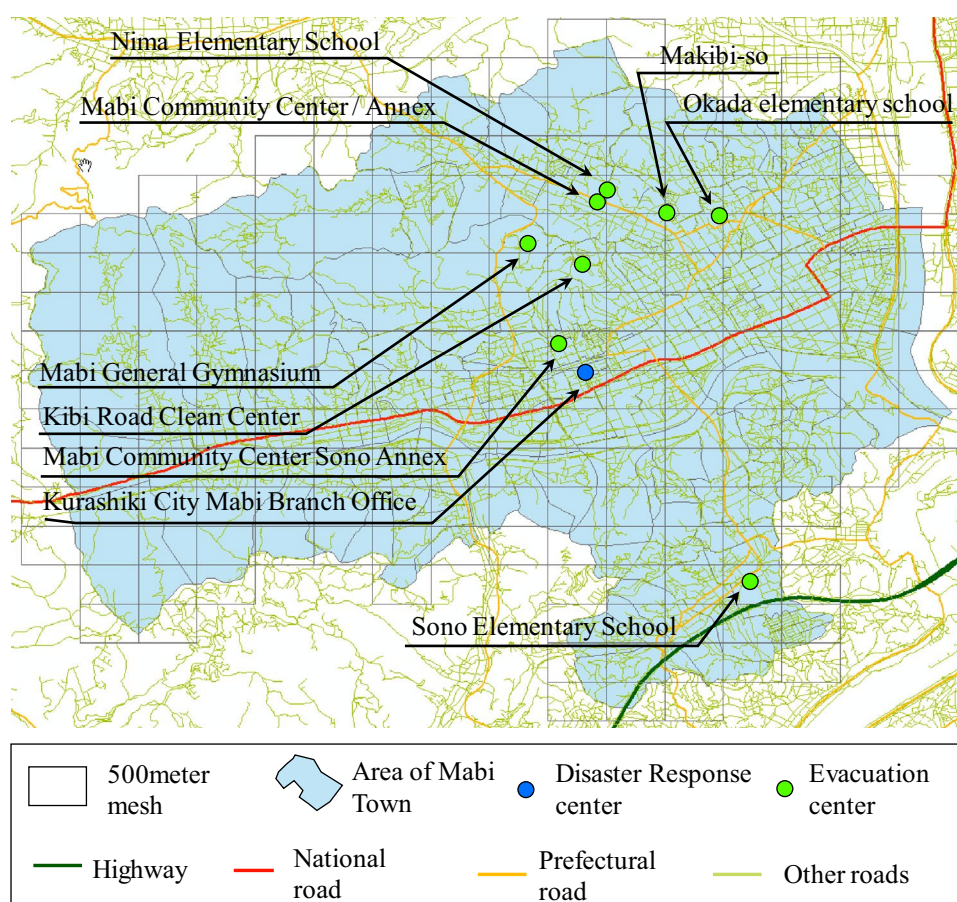
The road network data utilized in this study comes from the Conservation GIS consortium Japan [34]. In the case study area, there are 10,542 links and 8,422 nodes. The population flow data comes from the "Agoop Dinamic population data 500 m Mesh [35]." This data uses GPS location information collected from smartphones, which has been anonymized and statistically processed. It contains information on population density within 500-m mesh units for various periods. This study focuses on the data from July 2018 to analyze people's movements before and after the rainstorm to understand where individuals congregate immediately following a disaster.

3 Result and discussion

To demonstrate the superiority of the patrol method that utilizes population flow data, we first compare the total population at patrol points with that calculated using passive static data. In this context, a passive static patrol refers to disaster-stricken areas prioritized based on high population flow, using the 500-m mesh data from the 2020 national census.

Figure 7 illustrates the comparison results. The labels "10," "20," and "30" in the figure indicate the number of locations prioritized for patrols, starting from the mesh with the highest population flow. Since the disaster response center serves

Fig. 6 Mesh data and road network data



as both the starting and ending points of the tour, all eight evacuation centers are always visited. For instance, if the number of focusing locations based on population flow is ten, they are visited in order of population flow, in addition to the eight evacuation centers.

The term "Mobile data" in the figure refers to how the patrol route varies depending on the time of day, while "census data" remains constant regardless of the time. The vertical axis shows the total population of the location, calculated from the 500-m mesh of the population flow. Consequently, while the census-based route is consistent at any time, the population of the locations visited changes due to fluctuations in mobile data throughout the day. Table 1 shows an example of the calculation. The bottom of the table, 7,877 and 6,501, correspond to the red values in Fig. 7. At noon on July 7, the route based on population mobile data sums the populations of the top 20 locations, resulting in a total of 7,877. In contrast, the patrols based on census data are calculated using the top 20 locations from the census population ranking, yielding a total of 6,501.

Figure 7 indicates that the population data in the disaster area fluctuates during certain times, resulting in a total population that exceeds that of the census data. Furthermore, the total population in the disaster area similarly varies throughout the day for both datasets. For example, the total population at noon on the fifth and sixth is lower than other periods on the same days. A special warning was issued from the night of the 6th, after heavy rain, until 6:00 on the 8th; a decreasing trend in total population was observed across all periods.

Figure 8 presents the gap between mobile data and census data in the total population for patrolling. It reveals different trends between before and after the disaster. Specifically, before the disaster, the results for the ten locations tended to be more significant. For example, at noon on the 5th, there were 2,290 people at 10 locations, while 1,546 were at 30 locations at the same hour. Conversely, after the disaster, the results for the thirty locations tended to be larger. For example, the ten locations at noon on the 7th had a population of 1,096, whereas at 30 locations, it increased to 1,646. It illustrates that the population distribution changes before and after the disaster. It emphasizes the effectiveness of establishing patrol routes that consider the population dynamics after the disaster, which helps assess the situation of the roads connecting evacuation centers.

Fig. 7 Comparison of population along the patrol route

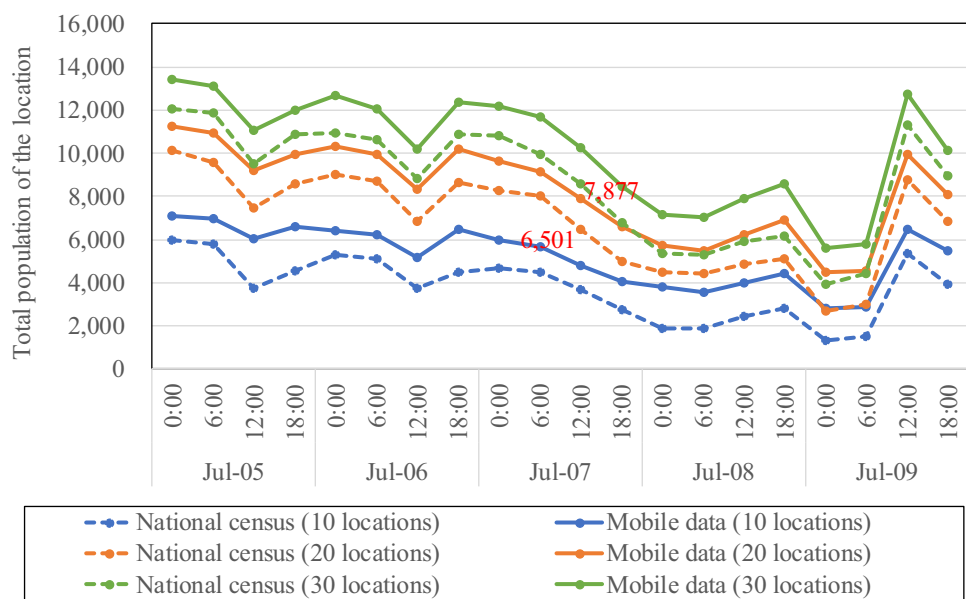
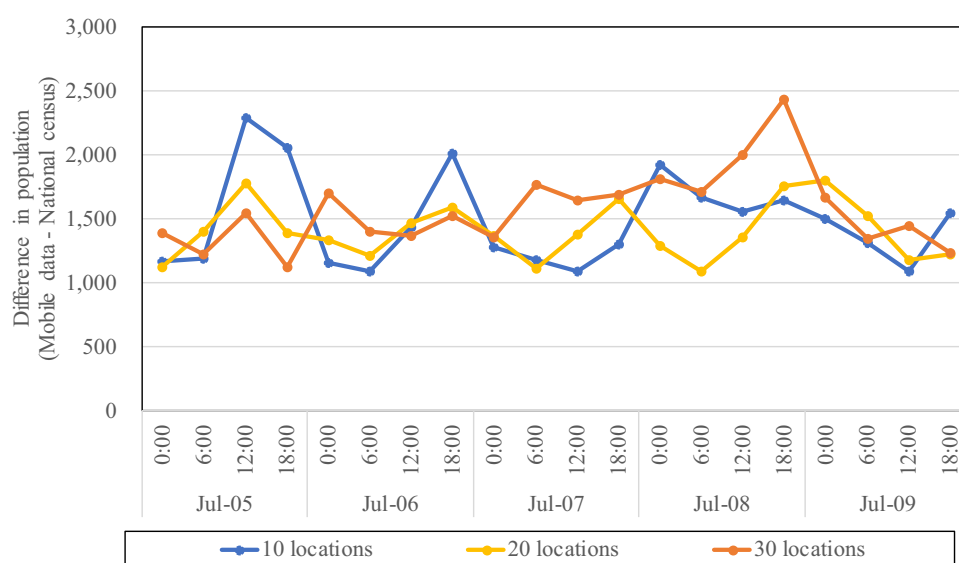


Table 1 Example of mesh population calculation for patrol

Rank	Target meshes based on mobile data		Target meshes based on national census		Mobile data corresponding to the ranking of the national census	
	Population at 12:00 on July 7th		National census		Population at 12:00 on July 7th	
	Rank	Population at 12:00 on July 7th	Rank	Population at 12:00 on July 7th	Rank	Population at 12:00 on July 7th
1	876		1	959	7	451
2	504		2	946	80	24
3	498		3	840	17	285
4	469		4	760	1	876
5	463		5	622	26	237
6	463		6	618	3	498
7	451		7	608	9	359
8	360		8	606	13	331
9	359		9	552	15	314
10	349		10	547	14	321
11	345		11	490	11	345
12	344		12	444	56	103
13	331		13	433	12	344
14	321		14	368	5	463
15	314		15	353	40	156
16	302		16	350	30	204
17	285		17	348	79	35
18	285		18	333	2	504
19	281		19	313	10	349
20	277		20	307	16	302
	7,877			10,797		6,501

Fig. 8 Deference between mobile data and national census along the Patrol Route



Next, an example of the visualized patrol routes can be seen in Fig. 9. The lower light panel shows the results of selecting 20 priority disaster areas from among the population-dense meshes, using the background of the 2020 national census 500-m mesh data and their corresponding patrol routes. The 100-m buffer around the patrol route signifies the area a UAV can cover from a height of 100 m. The remaining panels (top right, bottom left, bottom right) illustrate the patrol routes for the 20 priority disaster areas selected based on where the population is concentrated at different times (12:00, 18:00, and 0:00 on July 7th and 8th) according to the population flow data.

Figure 10 compares patrol routes with/ without a road network. The shortest path at noon on July 7 (represented by the blue line) is calculated using the Traveling Salesman Problem (TSP) based on the distance between nodes. However, this method does not account for the connectivity of land routes between nodes, making the results less applicable for evaluating the disaster situation. In contrast, the shortest path that considers the road network (denoted by the purple line) follows the roads between nodes, producing more relevant data for assessing the disaster situation.

Figure 9 shows that the areas with high population flow immediately after the disaster varied significantly depending on the time of day, which also influenced the patrol routes taken. For instance, at noon on the 7th, when the Odagawa River had breached its banks, and a unique heavy rain warning was in effect, the population was concentrated in the area east and south of Okada Elementary School, which served as an evacuation center. This observation aligns with the national census results. However, by 18:00 on the 7th and 0:00 on the 8th, the population began concentrating near the evacuation center (indicated by green nodes). This trend suggests that many individuals chose to remain close to their homes immediately following the flooding, but over time, more people started moving to evacuation centers. Despite this shift, the number of residents around the densely populated area near Okada Elementary School remained high, indicating that monitoring traffic conditions along the routes to evacuation centers could effectively guide residents.

Additionally, we organize the data collected from the patrol routes about road severance and road types. Figure 11 visualizes the results of overlapping road severance conditions with the data obtained from the patrol routes. The road segments depicted in the figure are those within the flood area published by the Geospatial Information Authority of Japan. Notably, even if a road is marked as "Disruption," it might still be passable depending on the depth of the flooding. The figure highlights that assessing the disruption status via land routes, such as by car, on the eastern side of the disaster response center was particularly challenging. Table 2 presents the results of the disruption status for the road segments based on patrol observations taken at different times post-disaster. This table breaks down the lengths of sections according to whether they were cut off, as shown in Fig. 9, specifically for roads that fall entirely (or partially) within the "100 m buffer of the patrol route" for each time indicated in Fig. 9. Approximately 40% of these road sections were disrupted at all times. If assessing the ground situation is complicated because these sections are impassable, using UAVs (drones) is expected to facilitate early situation assessment. Recent advances in deep learning technology have led to a growing number of research studies that utilize photographs taken from UAVs and other devices to assess road conditions [36–38]. This study's road conditions come from data from the Geospatial Information Authority of Japan; however, when applied to real-life disaster response scenarios, a road administrator can assess road conditions by deep learning techniques from aerial images from UAVs mentioned above.

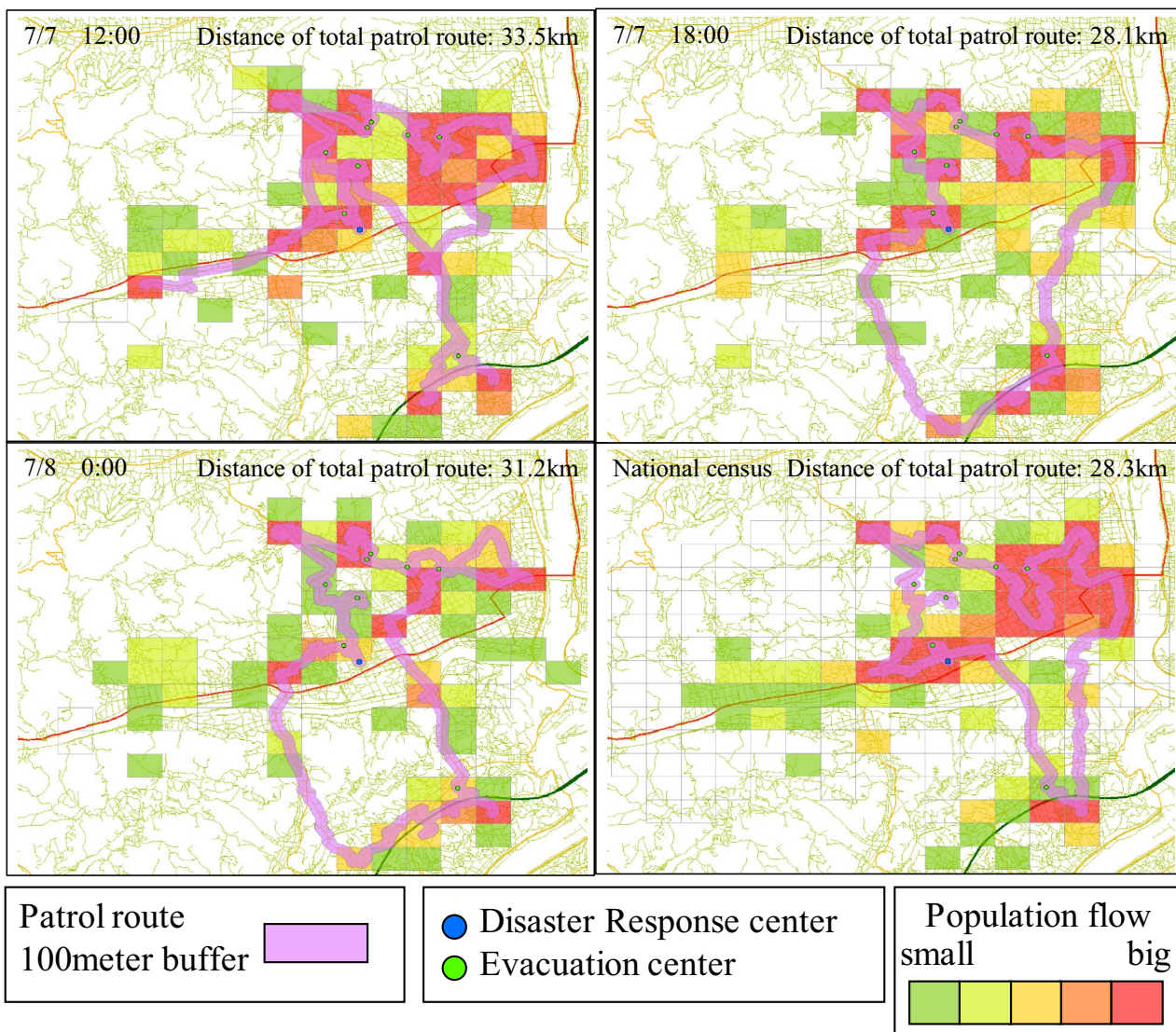


Fig. 9 Population flow and patrol routes

The second perspective, illustrated in Fig. 12 and Table 3, focuses on visualization and aggregation based on road type. This analysis reveals that 80–90% of the road sections surveyed by patrols were categorized as "other roads." Although these roads typically do not undergo road clearance operations, they are crucial for residents attempting to evacuate to shelters. Thus, early verification of the road severance situation could support quicker evacuations.

Finally, considering the route lengths, we evaluate the feasibility of patrolling the aforementioned routes using UAVs. The top right corner of each diagram in Fig. 9 displays the distance requiring patrol. Assuming a UAV with a maximum speed of 60 km/h and a maximum flight time of 40 minutes (the DJI Mavic3Pro has a maximum flight time of 43 minutes and a top speed of 75.6 km/h [39]), it is capable of continuously patrolling a distance of 40 km, exceeding all the distances presented in Fig. 9. Moreover, many UAVs available today can be programmed for automated flight along predetermined routes, and it is generally possible to ascertain whether patrolling a specific route is feasible. However, it is important to consider potential issues such as battery safety margins, the time needed for ascent and descent, route alterations, and the distance between the ground control and the aircraft.

Fig. 10 Comparison of patrol route with/without road network

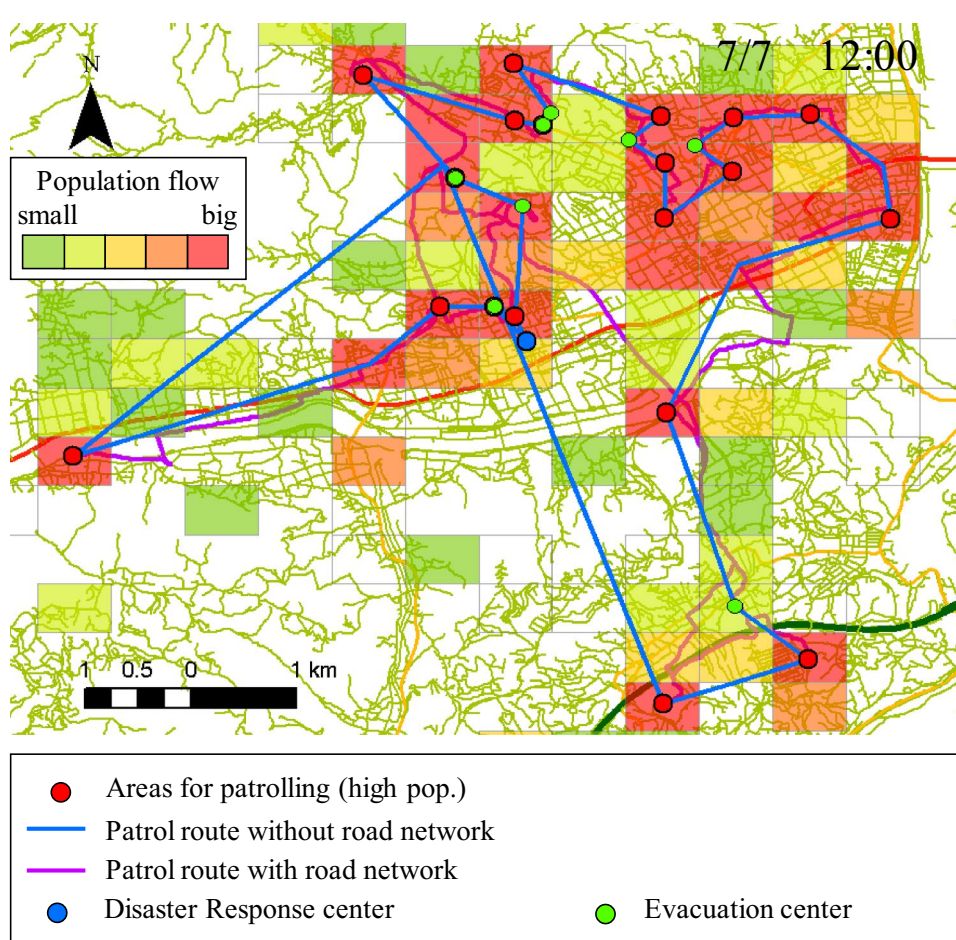


Fig. 11 Example of visualization of the patrol route and road condition

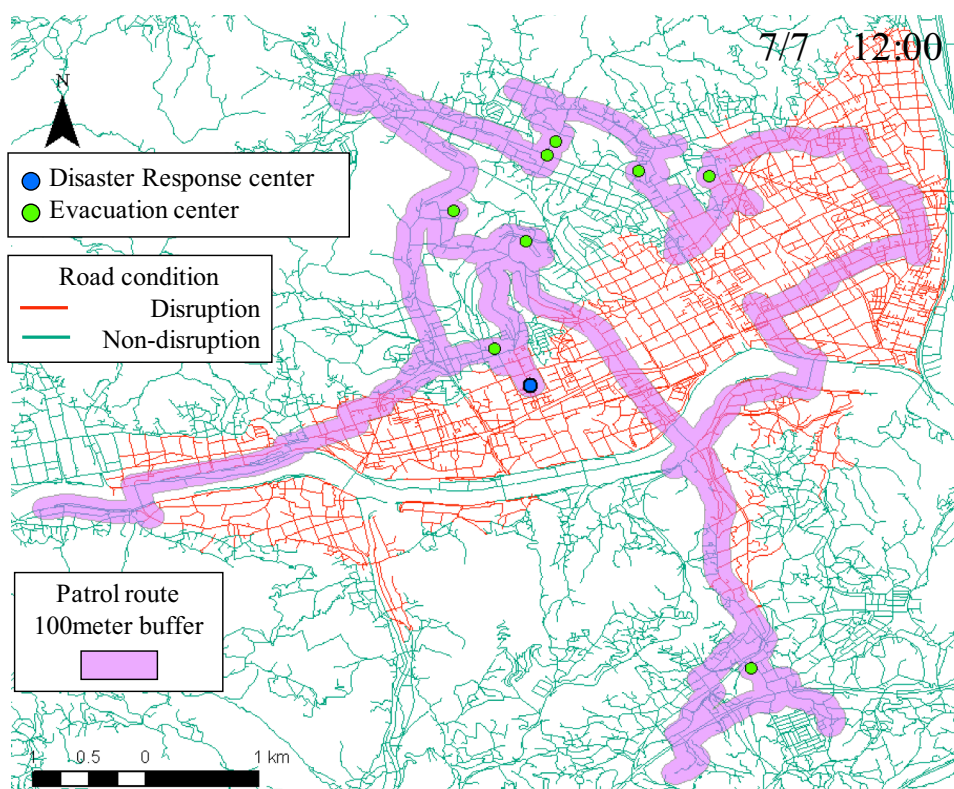
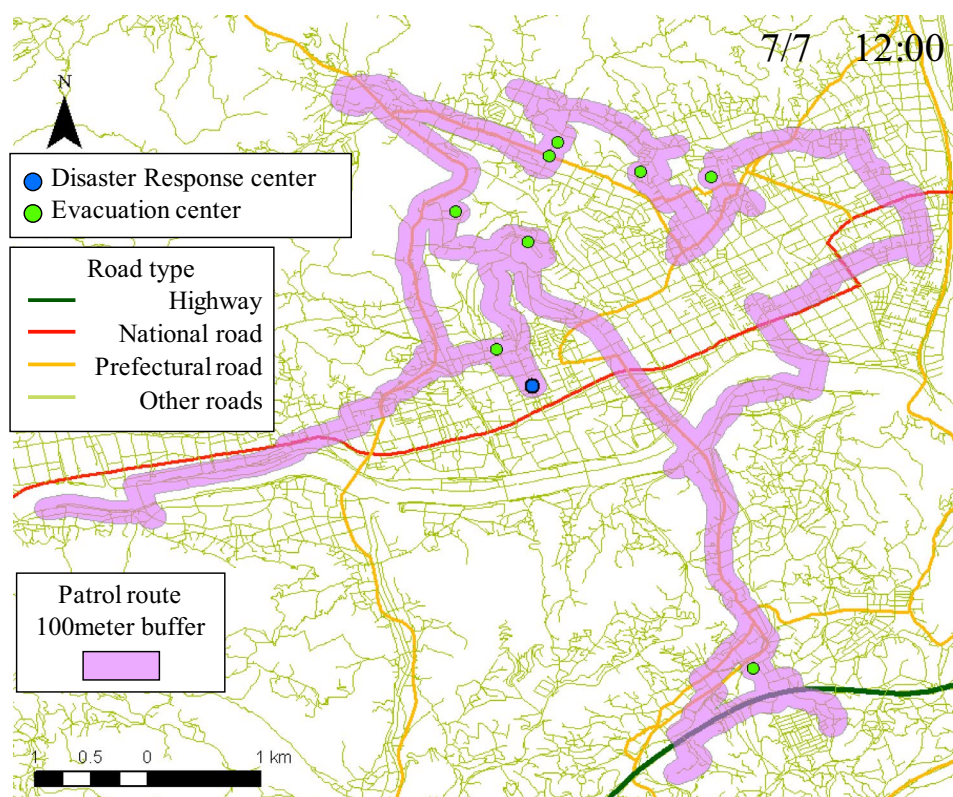


Table 2 The state of capturing road condition data during patrol

Date	Road length (Unit: kilometers)		
	Disruption	Non-disruption	
7/7 12:00	66.438	40%	98.404
7/7 18:00	54.527	37%	92.050
7/8 0:00	57.153	36%	102.572

Fig. 12 Example of visualization of the patrol route and road type**Table 3** The state of capturing road type data during patrol

Date	Highway (%)	National road (%)	Prefectural road (%)	Other roads (%)	Road length (Unit: kilometers)
7/7 12:00	2	1	8	89	165
7/7 18:00	2	1	7	90	147
7/8 0:00	2	1	11	86	160

4 Conclusion

International efforts to prevent, mitigate, and adapt to disasters are essential for safeguarding people's health and safety, protecting the environment, and ensuring a country's economic stability. These initiatives are supported by agreements such as the Sendai Framework for Disaster Risk Reduction, the United Nations Framework Convention on Climate Change (UNFCCC), and the Sustainable Development Goals (SDGs) [40]. After a disaster, various stakeholders collaborate to adapt to the situation and restore order, aiming to normalize the chaos. Quickly understanding the nature of the disaster enhances the ability to respond effectively.

Recent advances in digital transformation (DX) technology have sparked interest in new methods for disaster response. This research explores how UAVs and mobile data can be utilized in these efforts. Specifically, it examines how UAVs can be deployed to patrol disaster-affected areas with high population density during emergencies.

Applying this proposed method in Mabi town, Kurashiki City, Okayama Prefecture, which suffered significant damage from the July 2018 rains, demonstrated the ability to efficiently collect data on connectivity between disaster response center and disaster-stricken areas with high population concentrations. Additionally, it became evident that investigating the flooding of roads at the time was difficult by land routes, such as vehicles, since many routes, from populated areas to evacuation centers, were continuously flooded. This study conducted experiments at three specific times: noon on July 7, 6:00 p.m. on July 7, and midnight on July 8 as part of a case study. We developed patrol routes based on population distribution during the critical period immediately following the torrential rain when many residents began to evacuate. These findings offer valuable insights for municipal administrators responsible for road management, helping them determine the optimal moments to assess road blockage conditions.

Our study has some limitations. Regarding the disaster patrol method, the range of UAV patrols was limited, resulting in route outputs that did not prioritize certain roads. In cases of large-scale disasters, such as tsunamis, it is crucial to pre-select roads for repair in disaster response plans. Therefore, it is necessary to develop an algorithm that considers the disaster's scale by considering roads' functions for recovery. In addition, it is important to consider the issues of penetration and breakdown when utilizing population flow data. Regarding the penetration issue, communication companies provide population flow data with a low margin of error by multiplying the expansion coefficient. This coefficient is calculated by comparing the actual population with the ownership rate for each model. However, significant gaps can still occur in areas with low population [41, 42]. Regarding the breakdown issue, during the Noto Peninsula earthquake in 2024, mobile phone base stations operated by companies were rendered inoperable due to prolonged power outages from the disruption of transmission routes caused by landslides and other factors [43]. While assessing the second issue immediately after a disaster can be challenging, it is crucial to exercise caution when the population distribution deviates significantly from normal.

Author contributions The author conducted all the research work for this study.

Funding JSPS KAKENHI Grant Number 22K04580 supported this work.

Data availability The datasets generated for this study are not available in any online repository. On the other hand, the datasets generated by this work are available to the corresponding author and will be provided upon request.

Declarations

Ethics approval and consent to participate Not applicable. This manuscript does not involve research with human participants or animals.

Competing interests The authors declare no competing interests.

Open Access This article is licensed under a Creative Commons Attribution-NonCommercial-NoDerivatives 4.0 International License, which permits any non-commercial use, sharing, distribution and reproduction in any medium or format, as long as you give appropriate credit to the original author(s) and the source, provide a link to the Creative Commons licence, and indicate if you modified the licensed material. You do not have permission under this licence to share adapted material derived from this article or parts of it. The images or other third party material in this article are included in the article's Creative Commons licence, unless indicated otherwise in a credit line to the material. If material is not included in the article's Creative Commons licence and your intended use is not permitted by statutory regulation or exceeds the permitted use, you will need to obtain permission directly from the copyright holder. To view a copy of this licence, visit <http://creativecommons.org/licenses/by-nc-nd/4.0/>.

References

1. Kovács G, Spens KM. Humanitarian logistics in disaster relief operations. *Int J Phys Distrib Logist Manag.* 2007;37(2):99–114. <https://doi.org/10.1108/09600030710734820>.
2. Noyan N, Balcik B, Atakan S. A stochastic optimization model for designing last mile relief networks. *Transp Sci.* 2015;50(3):1092–113. <https://doi.org/10.1287/trsc.2015.0621>.
3. Alem D, Clark A, Moreno A. Stochastic network models for logistics planning in disaster relief. *Eur J Oper Res.* 2016;255(1):187–206. <https://doi.org/10.1016/j.ejor.2016.04.041>.

4. Zhang D, et al. Evaluation of a sensor system for detecting humans trapped under rubble: a pilot study. *Sensors*. 2018. <https://doi.org/10.3390/s18030852>.
5. Tuna G, Nefzi B, Conte G. Unmanned aerial vehicle-aided communications system for disaster recovery. *J Netw Comput Appl.* 2014;41:27–36. <https://doi.org/10.1016/j.jnca.2013.10.002>.
6. Bushnaq OM, Chaaban A, Al-Naffouri TY. The role of UAV-IoT networks in future wildfire detection. *IEEE Internet Things J.* 2021;8(23):16984–99. <https://doi.org/10.1109/JIOT.2021.3077593>.
7. Zhang R, et al. Automatic detection of earthquake-damaged buildings by integrating UAV oblique photography and infrared thermal imaging. *Remote Sens.* 2020. <https://doi.org/10.3390/rs12162621>.
8. Langhammer J, Vacková T. Detection and mapping of the geomorphic effects of flooding using UAV photogrammetry. *Pure Appl Geophys.* 2018;175(9):3223–45. <https://doi.org/10.1007/s00024-018-1874-1>.
9. Adsanver B, Coban E, Balcik B. A predictive multistage postdisaster damage assessment framework for drone routing. *Int Trans Oper Res.* 2025;32(2):626–68. <https://doi.org/10.1111/itor.13429>.
10. Reyes-Rubiano L, et al. Exploration of a disrupted road network after a disaster with an online routing algorithm. *OR Spectrum.* 2021;43(1):289–326. <https://doi.org/10.1007/s00291-020-00613-w>.
11. Qadir Z, Ullah F, Munawar HS, Al-Turjman F. Addressing disasters in smart cities through UAVs path planning and 5G communications: a systematic review. *Comput Commun.* 2021;168:114–35. <https://doi.org/10.1016/j.comcom.2021.01.003>.
12. Yabe T, Rao PSC, Ukkusuri SV, Cutter SL. Toward data-driven, dynamical complex systems approaches to disaster resilience. *Proc Natl Acad Sci.* 2022;119(8):e2111997119. <https://doi.org/10.1073/pnas.2111997119>.
13. Yabe T, et al. Understanding post-disaster population recovery patterns. *J R Soc Interface.* 2020;17(163):20190532. <https://doi.org/10.1098/rsif.2019.0532>.
14. Yamori K, Sugiyama T. Development and social implementation of smartphone app nige-tore for improving tsunami evacuation drills: synergistic effects between commitment and contingency. *Int J Disaster Risk Sci.* 2020;11(6):751–61. <https://doi.org/10.1007/s13753-020-00319-1>.
15. Yabe T, Sekimoto Y, Tsubouchi K, Ikemoto S. Cross-comparative analysis of evacuation behavior after earthquakes using mobile phone data. *PLoS ONE.* 2019;14(2):e0211375. <https://doi.org/10.1371/journal.pone.0211375>.
16. Lu X, et al. Unveiling hidden migration and mobility patterns in climate stressed regions: a longitudinal study of six million anonymous mobile phone users in Bangladesh. *Glob Environ Chang.* 2016;38:1–7. <https://doi.org/10.1016/j.gloenvcha.2016.02.002>.
17. Yabe T, Zhang Y, Ukkusuri SV. Quantifying the economic impact of disasters on businesses using human mobility data: a Bayesian causal inference approach. *EPJ Data Sci.* 2020;9(1):36. <https://doi.org/10.1140/epjds/s13688-020-00255-6>.
18. Daud MS, et al. Humanitarian logistics and its challenges: the literature review. *Int J Supply Chain Manag.* 2016;5:107–10.
19. Oruc BE, Kara BY. Post-disaster assessment routing problem. *Transp Res Part B Methodol.* 2018;116:76–102. <https://doi.org/10.1016/j.trb.2018.08.002>.
20. Shavigan R, Dong Z. Energy-Efficient Drone Coverage Path Planning using Genetic Algorithm. In: 2020 IEEE 21st International Conference on High Performance Switching and Routing (HPSR). 2020; 1–6. <https://doi.org/10.1109/HPSR48589.2020.9098989>
21. Chandran I, Vipin K. Multi-UAV networks for disaster monitoring: challenges and opportunities from a network perspective. *Drone Syst Appl.* 2024;12:1–28. <https://doi.org/10.1139/dsa-2023-0079>.
22. Aitsi-Selmi A, et al. Reflections on a science and technology agenda for 21st Century disaster risk reduction. *Int J Disaster Risk Sci.* 2016;7(1):1–29. <https://doi.org/10.1007/s13753-016-0081-x>.
23. Mens MJP, Klijn F, de Bruijn KM, van Beek E. The meaning of system robustness for flood risk management. *Environ Sci Policy.* 2011;14(8):1121–31. <https://doi.org/10.1016/j.envsci.2011.08.003>.
24. MATLAB. shortestpath. 2025. <https://www.mathworks.com/help/matlab/ref/graph.shortestpath.html>. Accessed 13 May 2025.
25. DANTZIG GB. Linear Programming and Extensions. Princeton University Press. 1991. <http://www.jstor.org/stable/j.ctt1cx3tvg>.
26. Geospatial Information Authority of Japan. Estimated color-coded map of the area around Mabi town, Kurashiki City during 2018 West Japan heavy rain. 2018. <https://www.gsi.go.jp/common/000208572.pdf>. Accessed 13 May 2025.
27. Kurashiki city. Report on the Disaster Response during during 2018 West Japan heavy rain. 2019. https://www.bousai.go.jp/fusugai/suigai_dosyaworking/pdf/kurashikikensyou.pdf. Accessed 13 May 2025.
28. Ministry of Land IT and T. Outline of 2018 West Japan heavy rain. 2018. <https://www.mlit.go.jp/common/001248491.pdf>. Accessed 13 May 2025.
29. Yoshida T, Hiroi K, Yamagata Y, Murakami D. Verification on Evacuation of Flood Disaster by Using Gps: Case Study in Mabi, Japan 2018. In: IGARSS 2019 - 2019 IEEE International Geoscience and Remote Sensing Symposium. 2019; 5633–5635. <https://doi.org/10.1109/IGARSS.2019.8898574>.
30. Kanemitsu N, Yamamoto H, Watanabe Y, Murakami H. The questionnaire survey on evacuation behavior for flood disaster by heavy rain event of July 2018 in Mabi, Kurashiki City. *J Disaster Sci Manag.* 2020;39:13–31. https://doi.org/10.24762/jndsj.39.S07_13.
31. Nishikawa S, Uchida O, Utsu K. Analysis of Rescue Request Tweets in the 2018 Japan Floods. In: Proceedings of the 2019 International Conference on Information Technology and Computer Communications. Association for Computing Machinery. 2019; 29–36. (ITCC '19). <https://doi.org/10.1145/3355402.3355408>.
32. Murakami H, Honoki S. Study on flood evacuation and geographical conditions in Mabi Area, Kurashiki City under the 2018 torrential rains in Western Japan – results of questionnaire survey. *J Soc Saf Sci.* 2019;35:153–62. <https://doi.org/10.11314/jisss.35.153>.
33. Kurashiki city. List of evacuation centers. 2025. <https://www.city.kurashiki.okayama.jp/3387.htm>. Accessed 13 May 2025.
34. Conservation GIS-consortium Japan. Top page. 2025. <http://cgisj.jp/>. Accessed 13 May 2025.
35. Agoop. Dinamic population data. 2025. <https://agoop.co.jp/service/dynamic-population-data/>. Accessed 13 May 2025.
36. Ahmad K, et al. Automatic detection of passable roads after floods in remote sensed and social media data. *Signal Process Image Commun.* 2019;74:110–8. <https://doi.org/10.1016/j.image.2019.02.002>.
37. Sakamoto J. Proposal of a flood damage road detection method based on deep learning and elevation data. *Geomat Nat Haz Risk.* 2024;15(1):2375545. <https://doi.org/10.1080/19475705.2024.2375545>.

38. Lopez-Fuentes L, et al. Deep learning models for road passability detection during flood events using social media data. *Appl Sci.* 2020. <https://doi.org/10.3390/app10248783>.
39. DJI. DJI Mini 4 Pro vs. DJI Air 3S vs. DJI Mavic 3 Pro. 2025. <https://store.dji.com/jp/content/dji-mini-4-pro-vs-dji-air-3s-vs-dji-mavic-3-pro>. Accessed 13 May 2025.
40. Siriwardana CSA, Jayasiri GP, Hettiarachchi SSL. Investigation of efficiency and effectiveness of the existing disaster management frameworks in Sri Lanka. *Proc Eng.* 2018;212:1091–8. <https://doi.org/10.1016/j.proeng.2018.01.141>.
41. Croce AI, Musolino G, Rindone C, Vitetta A. Estimation of travel demand models with limited information: floating car data for parameters' calibration. *Sustainability.* 2021. <https://doi.org/10.3390/su13168838>.
42. Shibukawa T, Asano S, Sogo K, Morimoto A. Study of indicator relating to the urban facility location plan using mobile spatial statistics -case study of Utsunomiya City. *J City Plan Inst Jpn.* 2018;53(3):408–15. <https://doi.org/10.11361/journalcpij.53.408>.
43. Ministry of Internal Affairs and Communications. Information and Communications White Paper. 2024. <https://www.soumu.go.jp/johotsusintokei/whitepaper/ja/r06/pdf/n1120000.pdf>.

Publisher's Note Springer Nature remains neutral with regard to jurisdictional claims in published maps and institutional affiliations.